Published in final edited form as:
Xenobiotica. 2013 November ; 43(11): 973–984. doi:10.3109/00498254.2013.791410.

Potential role of CYP2D6 in the central nervous system

Jie Cheng[1], **Yueying Zhen**[1], **Sharon Miksys**[2], **Diren Beyoğlu**[3], **Kristopher W. Krausz**[1], **Rachel F. Tyndale**[2], **Aiming Yu**[4], **Jeffrey R. Idle**[3], and **Frank J. Gonzalez**[1,*]

[1]Laboratory of Metabolism, Center for Cancer Research, National Cancer Institute, National Institutes of Health, Bethesda, MD 20892 [2]Centre for Addiction and Mental Health, Departments of Pharmacology & Toxicology and Psychiatry, University of Toronto, 1 King's College Circle, Toronto, Ontario, M5S 1A8 [3]Hepatology Research Group, Department of Clinical Research, University of Bern, 3010 Bern, Switzerland [4]Department of Pharmaceutical Science, University of Buffalo, Buffalo, NY 14214

Abstract

1. Cytochrome P450 2D6 (CYP2D6) is a pivotal enzyme responsible for a major human drug oxidation polymorphism in human populations. Distribution of CYP2D6 in brain and its role in serotonin metabolism suggest this CYP2D6 may have a function in central nervous system.
2. To establish an efficient and accurate platform for the study of CYP2D6 *in vivo*, a transgenic human CYP2D6 (Tg-2D6) model was generated by transgenesis in wild-type C57BL/6 (WT) mice using a P1 phage artificial chromosome clone containing the complete human CYP2D locus, including CYP2D6 gene and 5'- and 3'- flanking sequences.
3. Human CYP2D6 was expressed not only in the liver, but also in brain. The abundance of serotonin and 5-hydroxyindoleacetic acid in brain of Tg-2D6 is higher than in WT mice either basal levels or after harmaline induction. Metabolomics of brain homogenate and cerebrospinal fluid revealed a significant up-regulation of L-carnitine, acetyl-L-carnitine, pantothenic acid, dCDP, anandamide, *N*-acetylglucosaminylamine, and a down-regulation of stearoyl-L-carnitine in Tg-2D6 mice compared with WT mice. Anxiety tests indicate Tg-2D6 mice have a higher capability to adapt to anxiety.
4. Overall, these findings indicate that the Tg-2D6 mouse model may serve as a valuable *in vivo* tool to determine CYP2D6-involved neurophysiological metabolism and function.

Keywords

CYP2D6; brain; serotonin; anxiety

Introduction

Cytochrome P450 2D6 (CYP2D6), one of the most important enzymes involved in the metabolism of drugs, is characterized by a high inter-individual variability in catalytic

Correspondence: Frank J. Gonzalez, Laboratory of Metabolism, Center for Cancer Research, National Cancer Institute, Building 37, Room 3106, Bethesda, MD 20892. Telephone: (301) 496-9067. Fax: (301) 496-8419. fjgonz@helix.nih.gov.

Declaration of Interest
The authors have no conflicts of interest to report.

activity mainly caused by genetic polymorphism (Mahgoub et. al., 1977; Zanger et. al., 2004). Over a hundred drugs including antihypertensives, and many CNS acting drugs including antidepressants, neuroleptics and psychotropics (Brockmoller and Tzvetkov 2008) are mostly metabolized by CYP2D6. The prevalent CYP2D6 polymorphism in the human populations has led to multiple adverse drug reactions, even detrimental events, especially relative to the use of psychotropic and cardiovascular medications (Rau et. al., 2004). CYP2D6 metabolizers are mainly divided into poor metabolizers (PM), extensive metabolizers (EM), and ultra-extensive metabolizers, and to a limited degree intermediate metabolizers (Wijnen et. al., 2007) according to the activity and distribution of various CYP2D6 allelic variants.

Different activities of CYP2D6 in human populations have been correlated to different personality features of CYP2D6 PMs and CYP2D6 EMs; PMs were significantly more anxiety prone and less successful in socialization than EMs (Gan et. al., 2004; Iwashima et. al., 2007; Katoh et. al., 2007; Kim et. al., 2007; Roberts et. al., 2004; Suzuki et. al., 2003). CYP2D6 may influence metabolic activity in brain that in turn affects behavior. Deficiency of CYP2D6 was also reported to be related to generation of Parkinson's disease (Miksys and Tyndale 2006) and reduced CYP2D6 activity is inversely related to drug abuse dependence (Sellers et. al., 1997). Moreover, regeneration of serotonin from 5-methoxytryptamine by CYP2D6 revealed a possible important effect of CYP2D6 on neurophysiologic and pathophysiologic events (Yu et. al., 2003a). Serotonin is the fundamental neuromodulator in both vertebrate and invertebrate nervous systems and is the central neurotransmitter controlling impulsive and anxiety disorders (Kranz et. al., 2010). Thus, CYP2D6 is a potential influencing factor on the central nervous system as well as drug metabolism among the different human populations.

In the current study, a transgenic-CYP2D6 mouse (Tg-2D6) was established by transgenesis in C57BL/6 mice using a P1 artificial chromosome (PAC, BX247885) containing the complete human *CYP2D* locus to investigate CYP2D6 function. The expression of CYP2D6 was evaluated and the level of serotonin and its metabolites. Social anxiety tests were performed in Tg-2D6 and wild-type mice to determine the effect of CYP2D6 on social inclination. The present findings indicate that this mouse model may serve as a valuable *in vivo* tool to determine the role of CYP2D6 on brain metabolism and neurophysiological function.

Materials and methods

Animals

Male and female 8- to 9-week-old wild-type and Tg-2D6 mice were used in this study. All animals were maintained in an NCI animal facility under a standard 12 h light/12 h dark cycle with food and water supplied *ad libitum*. Handling and treatment of mice were performed in accordance with animal study protocols approved by the NCI Animal Care and Use Committee.

Materials

Debrisoquine, 4-hydroxydebrisoquine, harmaline, serotonin, 5-hydroxyindoleacetic acid (5-HIAA), HPLC-grade water, acetonitrile and formic acid were purchased from Sigma-Aldrich (St. Louis, MO). Debrisoquine was dissolved in isotonic saline (1.28 mg/ml) and at dose of 10 mg/kg and administered by oral gavage. Harmaline was dissolved in saline and administered at a dose of 20 mg/kg by *i.p.* injection (Wu et. al., 2009). Control mice were treated with saline, the vehicle for debrisoquine and harmaline administration.

Generation of the Tg-2D6 mouse

The CYP2D6 gene (Genbank accession number BX247885, PAC clone RP4-669P10) was microinjected into a fertilized FVB/N mouse eggs to produce a transgenic mouse line. Incorporation of the CYP2D6 genomic DNA within the mouse genome was determined by both PCR and Southern blot analysis. The transgenic founders were mated to a C57BL/6 mouse, and animals from this cross were subsequently crossed to C57BL/6 to produce homozygous mice. Mice homozygous for the transgene were confirmed by crossing them with wild-type (WT) mice and testing the progeny for transgene transmission. WT and homozygous littermates were bred and maintained by brother-sister mating.

PCR genotyping and southern blot analysis

Genomic DNA was isolated from tails as described as routine method. CYP2D6 gene-specific primers Sense 5'-AGAAGGGGAAGCAGGTTTG-3' and anti-sense 5'-CGGCACTCAGGACTAACTCATC-3', and microsomal epoxide hydrolase (Ephx1) gene-specific primers Sense 5'-AAGTGAGTTTGCATGGCGCAGC-3' and anti-sense 5'-CCCTTTAGCCCCTTCCCTCTG-3' were applied in CYP2D6 transgene detection. Mouse epoxide hydrolase (EH) gene primers served as a positive control for amplification. DNA was further digested with *Bam*HI and subjected to Southern blot analysis with DNA isolated from control and homozygous CYP2D6 transgenic mice.

Real-time PCR and western blot measurement

The specific primers for measurement of human CYP2D6 expression, excluding potential transcripts from the human CYP2D7 and CYP2D8P or mouse Cyp2d genes, were designed. Sense primer 5'AAAGGCTTTCCTGACCCAGC 3' and anti-sense primer 5' GTACCCATTCTAGCGGGG 3' were the optimal primers pairs. Tissue RNA extraction and reverse-transcription reaction were following routine method. β-Actin was chosen as the internal standard for gene quantization. For western blot analysis of CYP2D6 protein expression in liver, kidney, and intestine, tissues were homogenized in ice-cold buffer (1.15% KCl, 50 mM Tris-HCl, and 1 mM EDTA, pH 7.4) and microsomes were prepared by the method as described previously (Omura and Sato 1964a; Omura and Sato 1964b). Frontal cortex membranes were prepared from the frontal cortex by homogenizing in ice-cold buffer (adding protease inhibitor, Roche, Switzerland), followed by centrifugation at 3000×*g* for 5 min and centrifugation of the supernatant at 110,000×*g* for 90 min. Pellets were resuspended in 100 mM Tris (pH 7.4), 0.1 mM EDTA, 0.1 mM DTT, 1.15% w/v KCl, and 20% v/v glycerol, aliquoted, and stored at −80°C. MAB-2D6 (catalog No. 458246; BD Gentest, Woburn, MA) diluted 1:1000 with TBST, followed by peroxidase-conjugated anti-mouse IgG (Pierce Chemical Co., Rockford, IL) diluted 1:10,000 with TBST were used in western blot analysis. Glyceraldehyde 3-phosphate dehydrogenase (GAPDH) was used as an internal standard.

Immunohistochemistry of brain samples of Tg-2D6 and WT mice

Whole brains were fixed in 4% paraformaldehyde in phosphate buffer, cryoprotected in 20% sucrose, and 18 μm frozen sections were collected and stored in phosphate buffered saline. Coronal and longitudinal sections were immunostained with the M.O.M. (mouse on mouse from Vector Laboratories, Burlington, Canada) system according to the manufacturer's directions, followed by avidin-biotin complex (ABC, Vector Labs.) and 3,3'-diaminobenzidine (DAB, Vector Labs.) visualization. Monoclonal anti-CYP2D6 clone 4-74-1 (Gelboin et. al., 1997) was used at a concentration of 1:100 overnight at 4°C. Control sections were processed identically except for the omission of primary antibody. Digital images of brain sections from WT and Tg-2D6 mice were acquired at the same time under identical light and exposure conditions. Images of WT and Tg-2D6 brain sections were

grouped prior to any post-acquisition adjustment of contrast or brightness so that all images were adjusted identically.

Serotonin and 5-HIAA assays by HPLC

The brains of WT and Tg-2D6 mice were removed and washed with ice-cold saline (containing 40 μM pargyline). The brain was dried and weighed and a four-fold volume of ice-cold saline containing 40 μM pargyline was added and brains homogenized on ice and then stored at −80°C. Brain homogenate (50 μl) was removed and added to 450 μl of 0.1 M perchloric acid (PCA). After centrifugation at 14,000 rpm for 10 min at 4 °C, the supernatant was removed and injected for HPLC analysis. An Agilent 1100 series liquid chromatography including a vacuum degasser, a quaternary pump, an autosampler, a thermostatted column compartment, a DAD detector, and a fluorescence detector (Waldbronn, Germany) was controlled by ChemStation software. The samples processing conditions are as follows: Mobile phases: A 2% acetonitrile (0.02% trifluoroacetic acid), B 80% acetonitrile (0.02% trifluoroacetic acid), Column: Rechem Phenyl (4.6× 250 mm, 5 um), Flow rate: 1 mL/min, Gradient: 0–7 min 0%B-7%B, 7–18 min 7%B-40%B, 18–25 min 0%B, Injection volume: 25 μL; Excitation wavelength: 280 nm, Emission wavelength: 320 nm.

Pharmacokinetics analysis of mice treated with debrisoquine

Debrisoquine hemisulfate was dissolved in saline and administered by oral gavage at a dose of 10 mg/kg. For pharmacokinetic studies, blood samples were collected from suborbital veins 0, 0.5, 1, 2, 3, 4, 6, 8, 10, 12, and 24 h after debrisoquine administration. Each time point was analyzed with three to four animals. Serum was separated by centrifugation at 1000×g, 4°C, for 10 min. DEB and 4-OH-DEB were detected by LC-MS/MS. At the end of the experiments, mice were killed by carbon dioxide asphyxiation. Pharmacokinetic parameters for debrisoquine and 4-OH-DEB were estimated from the plasma concentration-concentration-time data by a noncompartmental approach using WinNonlin (Pharsight, Mountain View, CA). The maximum concentration in serum (C_{max}) was obtained from the original data. The area under the serum concentration-time curve ($AUC_{0–24}$) was calculated by the trapezoid rule.

Collection of biofluids and tissues from Tg-2D6 and WT mice

Twenty-four h urines of non-treated or debrisoquine treated Tg-2D6 mice and WT mice were collected by use of metabolic cages (Jencons, Leighton Buzzard, U.K.). Mice were killed by CO_2 asphyxiation 24 h after the last dose and sera were collected after urine collection by retro-orbital bleeding. Tissue samples (liver, hippocampus, frontal cortex, adrenal gland, cerebellum, lung, small intestine, prostate, kidney, heart, and spleen) were harvested and stored at −80°C before analysis. Brain (radias intersected evenly for the whole brain) of untreated Tg-2D6 and WT mice were homogenized in acetonitrile at 4°C. To collect cerebrospinal fluid, mice were anesthetized with 10 μg/ml ketamine ahead of surgery. Cisternal puncture was adopted for cerebrospinal fluid collection as described (Vogelweid and Kier 1988). Samples for ultraperformance liquid chromatography-electrospray ionization-quadrupole time-of-flight mass spectrometry (UPLC-ESI-QTOFMS) analysis were prepared by mixing 40 μl of urine with 160 μl of 50% acetonitrile, 2 μl cerebrospinal fluid with 98 μl of 50% acetonitrile and 5 μl of serum or tissue homogenate with 195 μl of 66% acetonitrile. Mixtures were centrifuged at 18,000 × g for 5 min to remove protein and particulates. Aliquots of the supernatant were transferred to autosampler vials for UPLC-ESI-QTOFMS analysis.

UPLC-ESI-QTOFMS based metabolomics

Aliquots (5 μl) of diluted biofluids and brain homogenate aliquot were injected into a Waters UPLC-ESI-QTOFMS system (Milford, MA). An Acquity UPLC™ BEH C18 column (Waters) was used to separate metabolites. The flow rate of the mobile phase was 0.6 ml/min with a gradient ranging from water to 95% aqueous acetonitrile containing 0.1% formic acid in a 10 min run. The QTOF Premier™ mass spectrometer was operated in both positive (ESI+) and negative (ESI−) electrospray ionization modes. Source temperature and desolvation temperature were set at 120 °C and 350 °C, respectively. Nitrogen was applied as the cone (50 l/h) and desolvation gas (600 l/h), and argon as collision gas. For accurate mass measurements, the QTOFMS was calibrated with sodium formate solution (range m/z 100–1000) and monitored by the intermittent injection of the lock mass sulfadimethoxine ($[M+H]^+$ = 311.0814 m/z; $[M-H]^-$ =309) in real time. Mass chromatograms and mass spectral data were acquired by MassLynx™ software in centroid format and deconvoluted using MarkerLynx™. Features were exported into SIMCA 13™ (Umetrics AB, Malmö, Sweden) for multivariate data analysis. Firstly, principal components analysis (PCA) was performed as this is an unsupervised analysis that provides a view of the internal structure of the dataset and the potential origins of the variances. In the PCA scores plot, which, in this case, shows a value for each mouse sample analyzed, a clustering of data for one type of mouse (i.e., male WT) and a separation from another type of mouse (male Tg-2D6) indicates a true difference in composition between the samples for each mouse type. Secondly, orthogonal partial least squares projection to latent structures-discriminant analysis (OPLS-DA) was performed, which is a supervised method that maximizes the difference between two groups of samples on one axis. The so-called OPLS-DA loadings S-plot is a convenient way of viewing, in this case, the ions that contribute to the separation between groups, in terms of both their relative abundance (X-axis) and their correlation to the model (Y-axis). Ions that are elevated in one group appear in one quadrant of the S-plot and those diminished in that group (and consequently elevated in the second group) appear in the opposite quadrant.

Behavioral tests

Harmaline-induced tremor score (Du and Harvey 1997), marble burying assay (Deacon 2006) and forced swimming test (FST) (Abel and Bilitzke 1990) were performed on WT and Tg-2D6 mice, using published methods. Each group of WT and Tg-2D6 mice had ten 2- to 3-month-old male adult mice for harmaline-induced tremor test and marble burying assay. Each group of WT and Tg-2D6 mice has 15 male adult mice of the same age for FST assay. In each assay, mice were observed on 1^{st}, 3^{rd}, 5^{th}, 7^{th} day after first training on 0 day. On 7^{th} day, mice were killed and tissues stored at −80°C.

Statistics

Experimental values are expressed as mean±standard deviation (SD). Statistical analysis was performed with two-tailed Student's t tests for unpaired data, and a P value of <0.05 considered as statistically significant.

Results

Effect of the CYP2D6 transgene on urinary metabolic phenotype

UPLC-ESI-QTOFMS metabolomics was employed to determine the effect of the *CYP2D6* transgene on the urinary metabolite profile of both untreated male and untreated female WT and Tg-2D6 mice and the same mice after administration of debrisoquine (10 mg/kg p.o.). These studies establish the extent to which the *CYP2D6* genotype influences their urinary metabolic phenotype. PCA scores plots revealed that neither in males nor in females did the

scores cluster and completely separate (Figure 1A). In both sexes, there was overlap between the scores for WT and Tg-2D6 mice, which can be interpreted as meaning that the urinary metabolite composition was altered little by *CYP2D6* genotype. However, the principal component of variance for the urinary ions detected by UPLC-ESI-QTOFMS (component 1) reflected the sex difference. However, when the mice were administered debrisoquine, there was little separation between female WT and Tg-2D6 mice, but a clear resolution of the urinary metabolomic phenotypes for the male mice (Figure 1B). OPLS-DA was then used to examine the effect of *CYP2D6* genotype on urinary metabolite profiles in male mice (Supplementary Figure 1). DEB appears as a prominent ion in the WT quadrant and 4-OH-DEB, together with two ring-opened metabolites ROM-1 and ROM-2, appearing in the Tg-2D6 quadrant of the S-plot. These ring-opened metabolites revealed in earlier studies (Allen et. al., 1976; Allen et. al., 1975; Idle et. al., 1979), arising from 1- and 3-hydroxylation of debrisoquine, are formed by CYP2D6 (Eiermann et. al., 1998). This more complex metabolomic phenotype involving DEB and three metabolites was previously suggested as an improved means of CYP2D6 phenotyping (Chen et. al., 2007). These findings clearly demonstrate that *CYP2D6* genotype determines urinary metabolomic phenotype after debrisoquine metabolism, especially in male mice, but CYP2D6 expression has little discernible effect on the urinary metabolomic phenotype of untreated animals.

CYP2D6 distribution in tissues

A *CYP2D6*-containing PAC clone was microinjected into FVB/N mouse eggs to produce a transgenic mouse line (Supplementary Figure 2A). Distinct from the previous transgenic-2D6 model (Corchero et. al., 2001), this PAC clone RP4–669P10 (Genbank, BX247885) on chromosome 22q13.31–13.33 contains the 3' end of pseudogene CYP2D8P1, the TCF20 gene for transcription factor 20, pseudogene CYP2D7P1, the CYP2D6 gene and three CpG islands. FVB/N female mice harboring the CYP2D6 transgene were crossed with male C57BL/6 mice and offspring crossed with C57BL/6 mice for at least six generations. Tg-2D6 mice in the heterozygous state on a C57BL/6 background were stable and Tg-2D6 mice made homozygous for the transgene were bred by brother-sister mating and homozygosity confirmed by crossing with WT mice and testing the progeny for transgene transmission among all offspring. Genotype analysis (Supplementary Figure 2B) and southern blot analysis (Supplementary Figure 2C) corresponds exactly with the predicted sizes calculated from the sequence of the CYP2D6 gene. Genotype results revealed that constitutive epoxide hydrolase gene (Ephx1) yielded a fragment of 341 bp in all samples. An additional band of 241 bp was amplified exclusively in Tg-2D6 animals.

Since human *CYP2D6* sequence has more than 80% sequence similarity with the mouse Cyp2d subfamily (Miksys et. al., 2005), sense and anti-sense primers were designed from 1811bp to 1551bp of the *CYP2D6* coding sequence. Quantitative real-time PCR results (n=6) revealed specific amplification of these primers with *CYP2D6* RNA but not mouse *Cyp2d* mRNAs. The relative expression of *CYP2D6* mRNA in Tg-2D6 mice followed the series of liver > hippocampus > frontal cortex> cerebellum > lung, small intestine, prostate, kidney, heart, and spleen, with liver showing an order of magnitude higher *CYP2D6* mRNA levels than the other tissues (Figure 2A). Notably was measureable expression of *CYP2D6* in the hippocampus, frontal cortex, and cerebellum. It was reported that CYP2D6 in human brain is localized in the pyramidal cells of the cortex and hippocampus and the Purkinje cells of the cerebellum (Siegle et. al., 2001). The results of expression of CYP2D6 in the brain of Tg-2D6 mice corresponded to the distribution described in human brain suggesting the potential for an important function for CYP2D6 in the central nervous system in humans. Western blot results further revealed that CYP2D6 protein was expressed in liver, kidney and intestine of Tg-2D6 mice with the expression in microsomes from the liver of the Tg-2D6 mice similar to that in human liver microsomes (Figure 2B, top pane). In agreement

with the mRNA data, CYP2D6 protein was expressed in the hippocampus, frontal cortex, and cerebellum (Figure 2B, bottom panel). No bands were detected in the liver or brains of WT mice using the anti-CYP2D6 antibody.

Immunohistochemistry results revealed that brain sections from WT mice were only faintly stained compared to control sections, suggesting that the monoclonal anti-human CYP2D6 had some, but very low, cross-reactivity with mouse CYP2Ds. Overall, the brains from Tg-2D6 mice showed more immunostaining than brains from WT mice. There is much more intense staining of the frontal cortex in transgenic compared to WT mice, parietal cortex pyramidal cells show strong immunoreactivity compared to no immunoreactivity in the same cells in WT mice (Figure 3A). The cytoplasmic bridges in the striatum (caudate-putamen) of Tg-2D6 mice were much more strongly stained than in WT mice (Figure 3B). In the striatal blood vessels, the endothelial lining shows strong CYP2D6 immunoreactivity in Tg-2D6 mice, with no immunoreactivity detected in WT mice (Figure 3B). In the cerebellum and hippocampus, the difference in immunoreactivity between transgenic and WT mice was evident but only moderate compared with frontal cortex and striatum (Figure 3C).

CYP2D6 expression in liver was confirmed by pharmacokinetic assays with debrisoquine (Blakey et. al., 2004) as a probe substrate (Supplementary Figure 3, Supplemental Table 1). 4-OH-DEB is the major monohydroxylated metabolite of debrisoquine produced by CYP2D6 in humans, dog and rat (Allen et. al., 1976). Mice were treated orally with 10 mg/kg debrisoquine. The maximal debrisoquine serum concentration (C_{max}) and $AUC_{0–24}$ of Tg-2D6 mice decreased 30% compared with WT mice treated with debrisoquine. The elimination half-life of debrisoquine was 1.5-times shorter in Tg-2D6 mice than WT control mice. However, the C_{max} value of 4-OH-DEB in Tg-2D6 mice is nearly 4-fold increased from that in WT mice and the $AUC_{0–24}$ value is 3-times higher than that of WT mice. These results reflect CYP2D6 metabolism of debrisoquine in liver, although different values were obtained for the new Tg-2D6 line compared with the values reported for the earlier Tg-2D6 line (Corchero et. al., 2001), but they shared the similar trend of decreased debrisoquine and increased 4-OH-DEB in plasma when compared with WT mice.

Analysis of serotonin and metabolites in brain of WT and Tg-2D6 mice

Since serotonin can be formed from 5-methoxytryptamine by CYP2D6 (Yu et. al., 2003a), expression of CYP2D6 in brain of Tg-2D6 mice would be expected to produce higher levels serotonin and its metabolites such as 5-HIAA. For the purposes of this study, the brain was divided into four parts, cerebellum, frontal cortex, hippocampus and the rest of the brain, and the same amount of brain tissues from WT and Tg-2D6 mice homogenized separately and the supernatants derived processed by HPLC. In addition, since harmaline is a canonical reversible monoamine oxidase A inhibitor, which can significantly increase serotonin levels (Winter et. al., 2011), the brain tissues from mice treated with harmaline were also analyzed. The results revealed that serotonin levels are significantly higher in various regions of the Tg-2D6 brain than in WT mice (Figure 4A). 5-HIAA is a principal terminal metabolite of serotonin and can be detected with serotonin in the same analysis (Kema et. al., 2000). 5-HIAA exhibited higher abundance in cerebellum, hippocampus, frontal cortex as well as rest of brain in Tg-2D6 mice than in WT mice (Figure 4B). Harmaline administration increased the abundance of serotonin by 20–30 fold compared to control, while decreasing 5-HIAA abundance in brain. Similarly, serotonin in cerebellum and rest of brain of Tg-2D6 was significantly higher than that in WT mice after harmaline administration and this was associated with higher levels of 5-HIAA in cerebellum and hippocampus of Tg-2D6 compared to WT mice.

The effect of the CYP2D6 transgene on brain and CSF metabolomes

Whole mouse brain homogenates were prepared and CSF collected and analyzed by UPLC-ESI-QTOFMS metabolomics using various in-house conditions for the analysis of serum and urine. For brain homogenate, 500 and 240 features in ESI+ and ESI− mode, respectively, were imported into SIMCA 13. For CSF, 115 to 258 and 75 to 116 features in ESI+ and ESI− mode, respectively, were imported into SIMCA 13. Projection to latent structures-discriminant analysis (PLS-DA) scores plots for both brain homogenate and CSF in both ESI+ and ESI− modes were then carried out (Figure 5). In all cases (panels A–D), Tg-2D6 and WT scores clustered and separated, indicating that the *CYP2D6* transgene likely had a significant impact of both brain and CSF metabolomes. To examine what ions most contributed to these separations, OPLS-DA analysis was undertaken and the loadings scatter S-plots (not shown) examined for ions with the greatest correlation (p(corr)[1]) to the OPLS-DA model (see above). For brain homogenate, three positive ions were highly correlated to the model, corresponding to pantothenic acid, L-carnitine and acetyl-L-carnitine, all of which are involved in β-oxidation of fatty acids (Table 1). Further analysis of these molecules using the raw UPLC-ESI-QTOFMS data in SIMCA 13, established that all three were highly statistically significantly elevated in the Tg-2D6 mouse brain homogenate relative to the WT mouse brain homogenate. Carnitine shuttles fatty acids into mitochondria and acetylcarnitine recycles carnitine to the cytosol, while pantothenic acid is used for CoA synthesis. Taken together, this would suggest that Tg-2D6 mouse brain has increased rates of fatty acid β-oxidation. However, it has long been known that rat brain mitochondria have limited β-oxidation capacity compared with heart mitochondria due to a low level of 3-oxoacyl-CoA thiolase (Yang et. al., 1987).

Similar metabolomic investigations were undertaken with CSF collected from Tg-2D6 and WT mice. Table 2 shows that for CSF, six ions were identified that were elevated in Tg-2D6 mice and two that were elevated in WT mice. Additionally, an ion with m/z=238.1006 and a retention time of 1.67 min was found, that corresponded to the $[M+H]^+$ adduct of ketamine, the anaesthetic used for the collection of CSF. Further analysis of the raw data revealed no statistically significant difference between the Tg-2D6 and WT mouse CSF in the ion currents for ketamine, thus providing a positive internal control. As with brain homogenate, carnitine was elevated in Tg-2D6 mouse CSF and, interestingly, stearoyl-L-carnitine was elevated in WT mouse CSF (attenuated in Tg-2D6 CSF). The quantitative and statistical evaluation of these molecules (Table 2) revealed that although deoxynucleotide dUMP did not reach statistical significance (P=0.078), it was included because it is a metabolite of dCDP arising from dCDP hydrolase (EC 3.6.1.12) and CMP deaminase (EC 3.5.4.12). dCDP showed a ~6-fold increase in Tg-2D6 CSF. This is of interest because dCDP-choline and dCDP-ethanolamine are involved in phospholipid biosynthesis (Kennedy et. al., 1959). There was a 2.5-fold increase in Tg-2D6 CSF in an ion corresponding to C6H12O6, which most likely is inositol, glucose, fructose or galactose. Further CSF samples were examined by GCMS after derivatization with methoxamine and BSTFA, which confirmed the presence of all four of these molecules in CSF (data not shown). However, it is not possible to conclude the nature of the elevated C6H12O6 at this time. *N*-Acetylglucosaminylamine (NAGAA) was tentatively identified as ~2-fold elevated in CSF of Tg-2D6 mice. When NAGAA is bound to asparagine, the enzyme glycosylasparaginase (EC 3.5.1.26) hydrolyses asparagine *in situ* to aspartate and releases NAGAA. Aspartylglucosamine accumulates when this enzyme is deficient leading to the lysosomal storage disease aspartylglucosaminuria (Dunder et. al., 2010). As for brain homogenate, carnitine was found to be elevated in Tg-2D6 mouse CSF (1.6-fold; P=0.018). Interestingly, stearoylcarnitine was reduced two-fold in Tg-2D6 CSF. Carnitine in the CSF of children was reported to be elevated due to meningitis and other neurological disorders (Shinawi et. al., 1998), but acylcarnitines were also elevated. The pattern observed here likely represents elevated brain

mitochondrial usage of fatty acids in Tg-2D6 mice. Citrate was elevated in Tg-2D6 mouse CSF (2.6-fold; P=0.025). The significance of this observation is unclear and citrate has been reported to occur in CSF at higher concentrations than in plasma (Hoffmann et. al., 1993). Finally, the endogenous cannabinoid neurotransmitter anandamide was found to be elevated in Tg-2D6 CSF (1.4-fold; P=0.038). This finding is somewhat puzzling since anandamide has been reported to be a CYP2D6 substrate (Sridar et. al., 2011).

Behavioral tests

Harmaline is one of the most frequently used tremorigenic drugs and harmaline-induced tremor is regarded as a model of essential tremor (Miwa 2007). The harmaline-induced tremor score was defined in 30 min as follows: levels ranging from 0 (no tremor) to 1 (intermediate head tremor), 2 (continuous head tremor), 3 (whole body tremor) and 4 (reduced tremor due to fatigue) (Du and Harvey 1997). The results revealed that a lower tremor score in Tg-2D6 mice (Figure 6A) is produced compared to WT mice that might be attributed to higher serotonin in the brain. In addition, the behavior anxiety tests including the marble burying assay and FST assay revealed that Tg-2D6 mice buried less marbles (Figure 6B) as well as having a longer swimming time (Figure 6C) compared to WT mice. From the 1^{st} to 7^{th} day, Tg-2D6 displayed similar activity on marble burying which was higher than the activity of WT mice. It was reported that marble burying/digging can be affected by any agent altering hippocampal function, including serotonin active compounds (Njung'e and Handley 1991). Less marbles buried indicates the activity of the serotonin cycle and attenuated anxiety, depression or obsessive-compulsive disorder to outside stress (Li et. al., 2006). The FST assay revealed that on 5^{th} and 7^{th} day, there are no significant differences between transgenic mice and WT mice, either in swimming time or floating time, coupling with increased floating time for both mice. It was reported that animals become more immobile the more they are exposed to the forced swimming test (Hawkins et. al., 1978). The different pattern of behavior response in Tg-2D6 and WT mice indicated that Tg-2D6 mice are less susceptible to anxiety compared with WT mice, which corresponds to increased serotonin levels via the serotonin-melatonin cycle (Yu et. al., 2003b) as a result of CYP2D6 expression in Tg-2D6 mice.

Discussion

CYP2D6 is a low-capacity, high-affinity enzyme (Yu et. al., 2004) that accounts for only a small percentage of liver P450 content but metabolizes a significant number of xenobiotic and endobiotic compounds. It was reported that CYP2D6 is involved in metabolism of over 100 drugs, most notably antipsychotic agents (Vandel et. al., 2007). A previous CYP2D6-humanized mouse line was produced using a lambda phage genomic clone containing the CYP2D6 gene. CYP2D6 was detected in the liver, kidney and small intestine (Corchero et. al., 2001). Since CYP2D6 is the important P450 in brain (Ferguson and Tyndale 2011), a new transgenic mouse line with a wider CYP2D6 tissue distribution was produced. A PAC clone containing the full gene locus and its regulatory elements was identified and used as a transgene. This PAC clone-transgenic line allowed for tissue-specific and inducible regulation of the transgene and thus is the preferred method for making a transgenic mouse that would be the most biologically predictive (Gonzalez 2004). Interestingly, the current results revealed that CYP2D6 mRNA and protein were expressed in multiple tissues, not only in liver, but also in extrahepatic tissues such as brain (cortex, hippocampus) in this transgenic line.

Metabolomics demonstrated that the urinary phenotype after debrisoquine metabolism was determined by the CYP2D6 transgene and this was confirmed by a plasma pharmacokinetic study. This established the expected hepatic functionality of the transgene. The appearance of elevated debrisoquine in urine and plasma in WT mice and prominent concentrations of

4-OH-DEB in urine and plasma, together with the two ring-opened metabolites in urine of Tg-2D6 mice was consistent with the published literature (Allen et. al., 1976; Allen et. al., 1975) (Chen et. al., 2007; Idle et. al., 1979).

Brain CYP2D6 expression in this model was established by protein and immunohistochemical analysis. The difference in staining intensity between WT and Tg-2D6 mice appears to vary among brain regions. This may be because of species differences in relative expression levels of CYP2D across brain regions. In both humans and mice the expression levels of CYP2D proteins are high in cerebellum, and low in hippocampus (Miksys et. al., 2005), resulting in less differential staining between transgenic and wild-type mice. In contrast, the relative expression levels of CYP2D protein in frontal cortex and striatum are high in humans but low in mice resulting in a more obvious difference in immunoreactivity. Moreover, serotonin and 5-HIAA are also higher and after induction by harmaline are increased further in brain of Tg-2D6 compared to WT mice. It was reported that reduced levels of serotonin and 5-HIAA strongly correlate with aggressive behavior and suicide by violent means in subgroups of young, male, personality-disordered subjects with seriously deviant behavior (Nantel-Vivier et. al., 2011). Thus, behavior tests were performed on the Tg-2D6 model. It is well known that β-carboline derivatives such as harmaline, harmine, and ibogaine can produce generalized tremor, with the tremor frequency likely to be higher in smaller animals (Yamazaki et. al., 1979). In particular, the rodent model of harmaline-induced tremor is widely used as an animal model of essential tremor, one of the most representative tremor disorders in humans (Deuschl and Elble 2000). The results revealed that Tg-2D6 mice had lower tremor than WT mice, which might be correlated with the higher serotonin levels in Tg-2D6 mice, as many reports suggest that serotonin synthesis inhibit olivocerebellar system and attenuate harmaline-induced tremors (Mehta et. al., 2003; Welsh et. al., 1998). The mice were also subjected to the marble burying test. Mice bury marbles because marbles evoked anxiety. Mice are naturally obsessive-compulsive (Njung'e and Handley 1991). Less marbles buried indicates more serotonin metabolism (Berendsen and Broekkamp 1990) and attenuated anxiety in Tg-2D6 mice. Tg-2D6 mice were also analyzed by the force swimming test (FST) assay that is the most widely used animal test predictive of antidepressant action (Abel and Bilitzke 1990). Serotonin selective reuptake inhibitors augment the serotonin level and reduce anxiety of mice, which display high mobility and low immobility status in the cylinder (Cryan et. al., 2005; Yamazaki et. al., 1979). Decrease in immobility of Tg-2D6 mice in 1st and 3rd day reflects a state of decreased fear or anxiety compared to WT mice. Therefore, these findings suggest that CYP2D6 might play the regulated role in serotonin metabolism and subsequently influence the anxiety inclination of Tg-2D6 and WT mice.

Given the clear neurochemical and behavioral differences between WT and Tg-2D6 mice described above, it was of interest to understand what discrete molecules, if any, might be altered in the brains and CSF of the transgenic mice. Therefore, UPLC-ESI-QTOFMS metabolomics was employed to investigate brain homogenates and CSF from the two mouse lines. It is of great interest that the three highly statistically significant up-regulated molecules in Tg-2D6 brain homogenate were L-carnitine, acetyl-L-carnitine and pantothenic acid. At first sight, it would appear that this indicated an increase in flux through mitochondrial fatty acid β-oxidation, as discussed above. However, it would appear that this process operates at a highly attenuated rate in the rodent brain (Yang et. al., 1987). Nevertheless, brain mitochondria, in parallel to a higher specific activity microsomal system, utilize saturated long-chain fatty acids for the synthesis of saturated very long-chain fatty acids that are incorporated into myelin (Bourre et. al., 1977). Based upon the available data, it is tempting to speculate that CoA-dependent fatty acid catabolism may be greater in the brains of Tg-2D6 mice, for reasons that are at present unclear. This proposition is

supported by the observation in Tg-2D6 CSF of higher L-carnitine and lower stearoyl-L-carnitine concentrations.

The synthesis of phosphatidylcholine and phosphatidylethanolamine glycerophospholipids provides the predominant biophysical scaffolds of membranes, including in the brain (Zarringhalam et. al., 2012). CDP-choline and CDP-ethanolamine, together with dCDP-choline and dCDP-ethanolamine can participate in the *de novo* synthesis of the respective glycerophospholipids (Kennedy et. al., 1959). Why dCDP was higher and its metabolite dUMP was lower in the CSF of Tg-2D6 mice is presently uncertain, but may reflect yet further differences in lipid metabolism in the brains of the transgenic mice.

Anandamide (*N*-arachidonylethanolamine) is an endocannabinoid, that is, an endogenous ligand of CB1 cannabinoid receptors in the central nervous system and CB2 cannabinoid receptors in the periphery. Anandamide is said to be strongly involved in anxiety and depression (Micale et. al., 2012). In fact, data from the forced swim test in rats combined with neurochemical analyses have been reported that suggest that endocannabinoid signaling may regulate serotonin neurotransmission in the prefrontal cortex and modulate stress coping behavior (McLaughlin et. al., 2012). Thus, elevated serotonin levels in the brains of Tg-2D6 mice reported here may have an impact on anandamide concentrations in Tg-2D6 mice. Anandamide has been reported to be converted to 20-hydroxyeicosatetraenoic acid ethanolamide and 14,15-epoxyeicosatetraenoic acid ethanolamide by CYP2D6 (Sridar et. al., 2011) and, as such, might be expected to occur at lower concentrations in the brains of Tg-2D6 mice. However, these pathways for anandamide catabolism are relatively minor compared with the major pathway of hydrolysis by fatty acid amide hydrolase (EC 3.5.1.99). The intersection of the serotonergic and endocannabinoid nervous systems in the brain with CYP2D6 is at present unknown, but the Tg-2D6 mouse line described here may play a significant role in deciphering these interactions.

There are a few concerns that need to be discussed concerning the validity of this model in determining the role of CYP2D6 in the brain. First is the impact of the endogenous mouse CYP2D enzymes. All findings in Tg-2D6 mice are directly compared with WT mice. While both mouse lines possess murine CYP2D enzymes, the metabolic and/or behavioral differences between the two mouse lines must surely be due to the effects of the transgene (or on another gene in or near the CYP2D6 gene cluster, see below). The mouse has no direct homologue to the human CYP2D6. While murine brain and liver microsomal preparations did show low-level activities in producing serotonin from 5-methoxytrptamine, this activity is highly CYP2D6 selective because the Tg-2D6 mouse showed much higher levels of serotonin produced from 5-methoxytrptamine both in vitro and in vivo as published in a earlier study (Yu et. al., 2003a).

It cannot be totally ruled out that some of the phenotypes obtained with the Tg-2D6 mice are due to the presence of the other genes within the in the PAC clone RP4–669P10 (Genbank, BX247885) used to generate this mouse line. TCF20, also called SPBP (stromelysin-1 PDGF1-responsive element-binding protein and AR1) is known to bind to the platelet-derived growth factor-responsive element in the matrix metalloproteinase 3 promoter, and to enhance the activity of transcription factors such as JUN and SP1 (Rajadhyaksha et. al., 1998; Rekdal et. al., 2000). However, wild-type mice should also express this factor and it is not clear what impact an extra copy of this protein would have on the chemical and behavioral differences observed in the present study. While other open reading frames for proteins or even microRNAs within this gene cluster may also be involved in the phenotype of the Tg-2D6 mice, most observations can be ascribed to the CYP2D6 gene.

Another concern of this study is the relative expression levels of brain CYP2D between wild-type mice and Tg-2D6 mice and humans. Unfortunately an accurate, direct interspecies comparison (WT vs either Tg-2D6 or human) would be difficult at this time, as the monoclonal antibody used for transgenic mice and humans does not detect wild-type mouse CYP2D, and there are no known antibodies selective for the various mouse CYP2D isoforms over CYP2D6 available to date. In addition, it is unknown which, if any, of the mouse Cyp2d isoforms are functionally homologous to human CYP2D6. We believe that mice have no homologue that shares the same activities and properties and CYP2D6. The data indicate that the estimated CYP2D6 expression per microgram of hepatic microsomal protein is comparable between livers of Tg-2D6 mice and humans in this and a previous study (Miksys et. al., 2005). From this we can estimate the brain CYP2D expression levels relative to the liver. For human cerebellum, expression is approximately 1% of hepatic levels (Miksys et. al., 2002). For Tg-2D6 mouse cerebellum, expression is approximately 20% of hepatic levels, moderately higher than in humans. This suggests that the Tg-2D6 model could be considered a brain overexpression model, but this remains to be verified.

In summary, CYP2D6 was found to have a critical role in the metabolism of endogenous neurochemicals through evaluation of Tg-2D6 mice and WT mice as illustrated in protein expression, debrisoquine metabolism, serotonin abundance and behavior tests. These data provide a mechanistic basis for novel therapies potentially targeting human CYP2D6 in brain disorders. Finally, the Tg-2D6 mouse model could not only be used as a platform to predict drug metabolism by CYP2D6 and shorten the process of drug discovery, but also open new vistas in brain research.

Supplementary Material

Refer to Web version on PubMed Central for supplementary material.

Acknowledgments

This study was supported by the National Cancer Institute Intramural Research Program, a CIHR grant MOP97751, CAMH and the Canada Foundation for Innovation (#20289 and #16014), the CAMH Foundation, and the Ontario Ministry of Research and Innovation.

References

Abel EL, Bilitzke PJ. A possible alarm substance in the forced swimming test. Physiol Behav. 1990; 48:233–239. [PubMed: 2255725]

Allen JG, Brown AN, Marten TR. Metabolism of debrisoquine sulphate in rat, dog and man. Xenobiotica. 1976; 6:405–409. [PubMed: 997588]

Allen JG, East PB, Francis RJ, Haigh JL. Metabolism of debrisoquine sulfate. Identification of some urinary metabolites in rat and man. Drug Metab Dispos. 1975; 3:332–337. [PubMed: 241613]

Berendsen HH, Broekkamp CL. Behavioural evidence for functional interactions between 5-HT-receptor subtypes in rats and mice. Br J Pharmacol. 1990; 101:667–673. [PubMed: 2150180]

Blakey GE, Lockton JA, Perrett J, Norwood P, Russell M, Aherne Z, Plume J. Pharmacokinetic and pharmacodynamic assessment of a five-probe metabolic cocktail for CYPs 1A2, 3A4, 2C9, 2D6 and 2E1. Br J Clin Pharmacol. 2004; 57:162–169. [PubMed: 14748815]

Bourre JM, Paturneau-Jouas MY, Daudu OL, Baumann NA. Lignoceric acid biosynthesis in the developing brain. Activities of mitochondrial acetyl-CoA-dependent synthesis and microsomal malonyl-CoA chain-elongating system in relation to myelination. Comparison between normal mouse and dysmyelinating mutants (quaking and jimpy). Eur J Biochem. 1977; 72:41–47. [PubMed: 836393]

Brockmoller J, Tzvetkov MV. Pharmacogenetics: data, concepts and tools to improve drug discovery and drug treatment. Eur J Clin Pharmacol. 2008; 64:133–157. [PubMed: 18224312]

Chen C, Gonzalez FJ, Idle JR. LC-MS-based metabolomics in drug metabolism. Drug Metab Rev. 2007; 39:581–597. [PubMed: 17786640]

Corchero J, Granvil CP, Akiyama TE, Hayhurst GP, Pimprale S, Feigenbaum L, Idle JR, Gonzalez FJ. The CYP2D6 humanized mouse: effect of the human CYP2D6 transgene and HNF4alpha on the disposition of debrisoquine in the mouse. Mol Pharmacol. 2001; 60:1260–1267. [PubMed: 11723233]

Cryan JF, Valentino RJ, Lucki I. Assessing substrates underlying the behavioral effects of antidepressants using the modified rat forced swimming test. Neurosci Biobehav Rev. 2005; 29:547–569. [PubMed: 15893822]

Deacon RM. Digging and marble burying in mice: simple methods for in vivo identification of biological impacts. Nat Protoc. 2006; 1:122–124. [PubMed: 17406223]

Deuschl G, Elble RJ. The pathophysiology of essential tremor. Neurology. 2000; 54:S14–S20. [PubMed: 10854347]

Du W, Harvey JA. Harmaline-induced tremor and impairment of learning are both blocked by dizocilpine in the rabbit. Brain Res. 1997; 745:183–188. [PubMed: 9037408]

Dunder U, Valtonen P, Kelo E, Mononen I. Early initiation of enzyme replacement therapy improves metabolic correction in the brain tissue of aspartylglycosaminuria mice. J Inherit Metab Dis. 2010; 33:611–617. [PubMed: 20607610]

Eiermann B, Edlund PO, Tjernberg A, Dalen P, Dahl ML, Bertilsson L. 1- and 3-hydroxylations, in addition to 4-hydroxylation, of debrisoquine are catalyzed by cytochrome P450 2D6 in humans. Drug Metab Dispos. 1998; 26:1096–1101. [PubMed: 9806952]

Ferguson CS, Tyndale RF. Cytochrome P450 enzymes in the brain: emerging evidence of biological significance. Trends Pharmacol Sci. 2011; 32:708–714. [PubMed: 21975165]

Gan SH, Ismail R, Wan Adnan WA, Zulmi W, Kumaraswamy N, Larmie ET. Relationship between Type A and B personality and debrisoquine hydroxylation capacity. Br J Clin Pharmacol. 2004; 57:785–789. [PubMed: 15151524]

Gelboin HV, Krausz KW, Shou M, Gonzalez FJ, Yang TJ. A monoclonal antibody inhibitory to human P450 2D6: a paradigm for use in combinatorial determination of individual P450 role in specific drug tissue metabolism. Pharmacogenetics. 1997; 7:469–477. [PubMed: 9429232]

Gonzalez FJ. Cytochrome P450 humanised mice. Hum Genomics. 2004; 1:300–306. [PubMed: 15588489]

Hawkins J, Hicks RA, Phillips N, Moore JD. Swimming rats and human depression. Nature. 1978; 274:512–513. [PubMed: 672980]

Hoffmann GF, Meier-Augenstein W, Stockler S, Surtees R, Rating D, Nyhan WL. Physiology and pathophysiology of organic acids in cerebrospinal fluid. J Inherit Metab Dis. 1993; 16:648–669. [PubMed: 8412012]

Idle JR, Mahgoub A, Angelo MM, Dring LG, Lancaster R, Smith RL. The metabolism of [14C]-debrisoquine in man. Br J Clin Pharmacol. 1979; 7:257–266. [PubMed: 371651]

Iwashima K, Yasui-Furukori N, Kaneda A, Saito M, Nakagami T, Sato Y, Kaneko S. No association between CYP2D6 polymorphisms and personality trait in Japanese. Br J Clin Pharmacol. 2007; 64:96–99. [PubMed: 17324244]

Katoh M, Sawada T, Soeno Y, Nakajima M, Tateno C, Yoshizato K, Yokoi T. In vivo drug metabolism model for human cytochrome P450 enzyme using chimeric mice with humanized liver. J Pharm Sci. 2007; 96:428–437. [PubMed: 17051594]

Kema IP, de Vries EG, Muskiet FA. Clinical chemistry of serotonin and metabolites. J Chromatogr B Biomed Sci Appl. 2000; 747:33–48. [PubMed: 11103898]

Kennedy EP, Borkenhagen LF, Smith SW. Possible metabolic functions of deoxycytidine diphosphate choline and deoxycytidine diphosphate ethanolamine. The Journal of biological chemistry. 1959; 234:1998–2000. [PubMed: 13673002]

Kim E, Levy R, Pikalov A. Personalized treatment with atypical antipsychotic medications. Adv Ther. 2007; 24:721–740. [PubMed: 17901022]

Kranz GS, Kasper S, Lanzenberger R. Reward and the serotonergic system. Neuroscience. 2010; 166:1023–1035. [PubMed: 20109531]

Li X, Morrow D, Witkin JM. Decreases in nestlet shredding of mice by serotonin uptake inhibitors: comparison with marble burying. Life Sci. 2006; 78:1933–1939. [PubMed: 16182315]

Mahgoub A, Idle JR, Dring LG, Lancaster R, Smith RL. Polymorphic hydroxylation of Debrisoquine in man. Lancet. 1977; 2:584–586. [PubMed: 71400]

McLaughlin RJ, Hill MN, Bambico FR, Stuhr KL, Gobbi G, Hillard CJ, Gorzalka BB. Prefrontal cortical anandamide signaling coordinates coping responses to stress through a serotonergic pathway. Eur Neuropsychopharmacol. 2012; 22:664–671. [PubMed: 22325231]

Mehta H, Saravanan KS, Mohanakumar KP. Serotonin synthesis inhibition in olivo-cerebellar system attenuates harmaline-induced tremor in Swiss albino mice. Behav Brain Res. 2003; 145:31–36. [PubMed: 14529803]

Micale V, Di Marzo V, Sulcova A, Wotjak CT, Drago F. Endocannabinoid system and mood disorders: Priming a target for new therapies. Pharmacol Ther. 2012

Miksys S, Rao Y, Hoffmann E, Mash DC, Tyndale RF. Regional and cellular expression of CYP2D6 in human brain: higher levels in alcoholics. Journal of neurochemistry. 2002; 82:1376–1387. [PubMed: 12354285]

Miksys S, Tyndale RF. Nicotine induces brain CYP enzymes: relevance to Parkinson's disease. J Neural Transm Suppl. 2006:177–180. [PubMed: 17017527]

Miksys SL, Cheung C, Gonzalez FJ, Tyndale RF. Human CYP2D6 and mouse CYP2Ds: organ distribution in a humanized mouse model. Drug Metab Dispos. 2005; 33:1495–1502. [PubMed: 16033950]

Miwa H. Rodent models of tremor. Cerebellum. 2007; 6:66–72. [PubMed: 17366267]

Nantel-Vivier A, Pihl RO, Young SN, Parent S, Belanger SA, Sutton R, Dubois ME, Tremblay RE, Seguin JR. Serotonergic contribution to boys' behavioral regulation. Plos One. 2011; 6:e20304. [PubMed: 21673801]

Njung'e K, Handley SL. Evaluation of marble-burying behavior as a model of anxiety. Pharmacol Biochem Behav. 1991; 38:63–67. [PubMed: 2017455]

Omura T, Sato R. The Carbon Monoxide-Binding Pigment of Liver Microsomes. I. Evidence for Its Hemoprotein Nature. The Journal of biological chemistry. 1964a; 239:2370–2378. [PubMed: 14209971]

Omura T, Sato R. The Carbon Monoxide-Binding Pigment of Liver Microsomes. Ii. Solubilization, Purification, and Properties. The Journal of biological chemistry. 1964b; 239:2379–2385. [PubMed: 14209972]

Rajadhyaksha A, Riviere M, Van Vooren P, Szpirer J, Szpirer C, Babin J, Bina M. Assignment of AR1, transcription factor 20 (TCF20), to human chromosome 22q13.3 with somatic cell hybrids and in situ hybridization. Cytogenetics and cell genetics. 1998; 81:176–177. [PubMed: 9730594]

Rau T, Wohlleben G, Wuttke H, Thuerauf N, Lunkenheimer J, Lanczik M, Eschenhagen T. CYP2D6 genotype: impact on adverse effects and nonresponse during treatment with antidepressants-a pilot study. Clin Pharmacol Ther. 2004; 75:386–393. [PubMed: 15116051]

Rekdal C, Sjottem E, Johansen T. The nuclear factor SPBP contains different functional domains and stimulates the activity of various transcriptional activators. The Journal of biological chemistry. 2000; 275:40288–40300. [PubMed: 10995766]

Roberts RL, Luty SE, Mulder RT, Joyce PR, Kennedy MA. Association between cytochrome P450 2D6 genotype and harm avoidance. Am J Med Genet B Neuropsychiatr Genet. 2004; 127B:90–93. [PubMed: 15108188]

Sellers EM, Otton SV, Tyndale RF. The potential role of the cytochrome P-450 2D6 pharmacogenetic polymorphism in drug abuse. NIDA Res Monogr. 1997; 173:6–26. [PubMed: 9260180]

Shinawi M, Gruener N, Lerner A. CSF levels of carnitine in children with meningitis, neurologic disorders, acute gastroenteritis, and seizure. Neurology. 1998; 50:1869–1471. [PubMed: 9633746]

Siegle I, Fritz P, Eckhardt K, Zanger UM, Eichelbaum M. Cellular localization and regional distribution of CYP2D6 mRNA and protein expression in human brain. Pharmacogenetics. 2001; 11:237–245. [PubMed: 11337939]

Sridar C, Snider NT, Hollenberg PF. Anandamide oxidation by wild-type and polymorphically expressed CYP2B6 and CYP2D6. Drug Metab Dispos. 2011; 39:782–788. [PubMed: 21289075]

Suzuki E, Kitao Y, Ono Y, Iijima Y, Inada T. Cytochrome P450 2D6 polymorphism and character traits. Psychiatr Genet. 2003; 13:111–113. [PubMed: 12782969]

Vandel P, Talon JM, Haffen E, Sechter D. Pharmacogenetics and drug therapy in psychiatry--the role of the CYP2D6 polymorphism. Curr Pharm Des. 2007; 13:241–250. [PubMed: 17269931]

Vogelweid CM, Kier AB. A technique for the collection of cerebrospinal fluid from mice. Lab Anim Sci. 1988; 38:91–92. [PubMed: 3367632]

Welsh JP, Chang B, Menaker ME, Aicher SA. Removal of the inferior olive abolishes myoclonic seizures associated with a loss of olivary serotonin. Neuroscience. 1998; 82:879–897. [PubMed: 9483543]

Wijnen PA, Op den Buijsch RA, Drent M, Kuijpers PM, Neef C, Bast A, Bekers O, Koek GH. Review article: The prevalence and clinical relevance of cytochrome P450 polymorphisms. Aliment Pharmacol Ther. 2007; 26(Suppl 2):211–219. [PubMed: 18081664]

Winter JC, Amorosi DJ, Rice KC, Cheng K, Yu AM. Stimulus control by 5-methoxy-N,N-dimethyltryptamine in wild-type and CYP2D6-humanized mice. Pharmacol Biochem Behav. 2011; 99:311–315. [PubMed: 21624387]

Wu C, Jiang XL, Shen HW, Yu AM. Effects of CYP2D6 status on harmaline metabolism, pharmacokinetics and pharmacodynamics, and a pharmacogenetics-based pharmacokinetic model. Biochemical pharmacology. 2009; 78:617–624. [PubMed: 19445902]

Yamazaki M, Tanaka C, Takaori S. Significance of central noradrenergic system on harmaline induced tremor. Pharmacol Biochem Behav. 1979; 10:421–427. [PubMed: 450952]

Yang SY, He XY, Schulz H. Fatty acid oxidation in rat brain is limited by the low activity of 3-ketoacyl-coenzyme A thiolase. The Journal of biological chemistry. 1987; 262:13027–13032. [PubMed: 3654601]

Yu AM, Idle JR, Byrd LG, Krausz KW, Kupfer A, Gonzalez FJ. Regeneration of serotonin from 5-methoxytryptamine by polymorphic human CYP2D6. Pharmacogenetics. 2003a; 13:173–181. [PubMed: 12618595]

Yu AM, Idle JR, Gonzalez FJ. Polymorphic cytochrome P450 2D6: humanized mouse model and endogenous substrates. Drug Metab Rev. 2004; 36:243–277. [PubMed: 15237854]

Yu AM, Idle JR, Herraiz T, Kupfer A, Gonzalez FJ. Screening for endogenous substrates reveals that CYP2D6 is a 5-methoxyindolethylamine O-demethylase. Pharmacogenetics. 2003b; 13:307–319. [PubMed: 12777961]

Zanger UM, Raimundo S, Eichelbaum M. Cytochrome P450 2D6: overview and update on pharmacology, genetics, biochemistry. Naunyn Schmiedebergs Arch Pharmacol. 2004; 369:23–37. [PubMed: 14618296]

Zarringhalam K, Zhang L, Kiebish MA, Yang K, Han X, Gross RW, Chuang J. Statistical analysis of the processes controlling choline and ethanolamine glycerophospholipid molecular species composition. PLoS One. 2012; 7:e37293. [PubMed: 22662143]

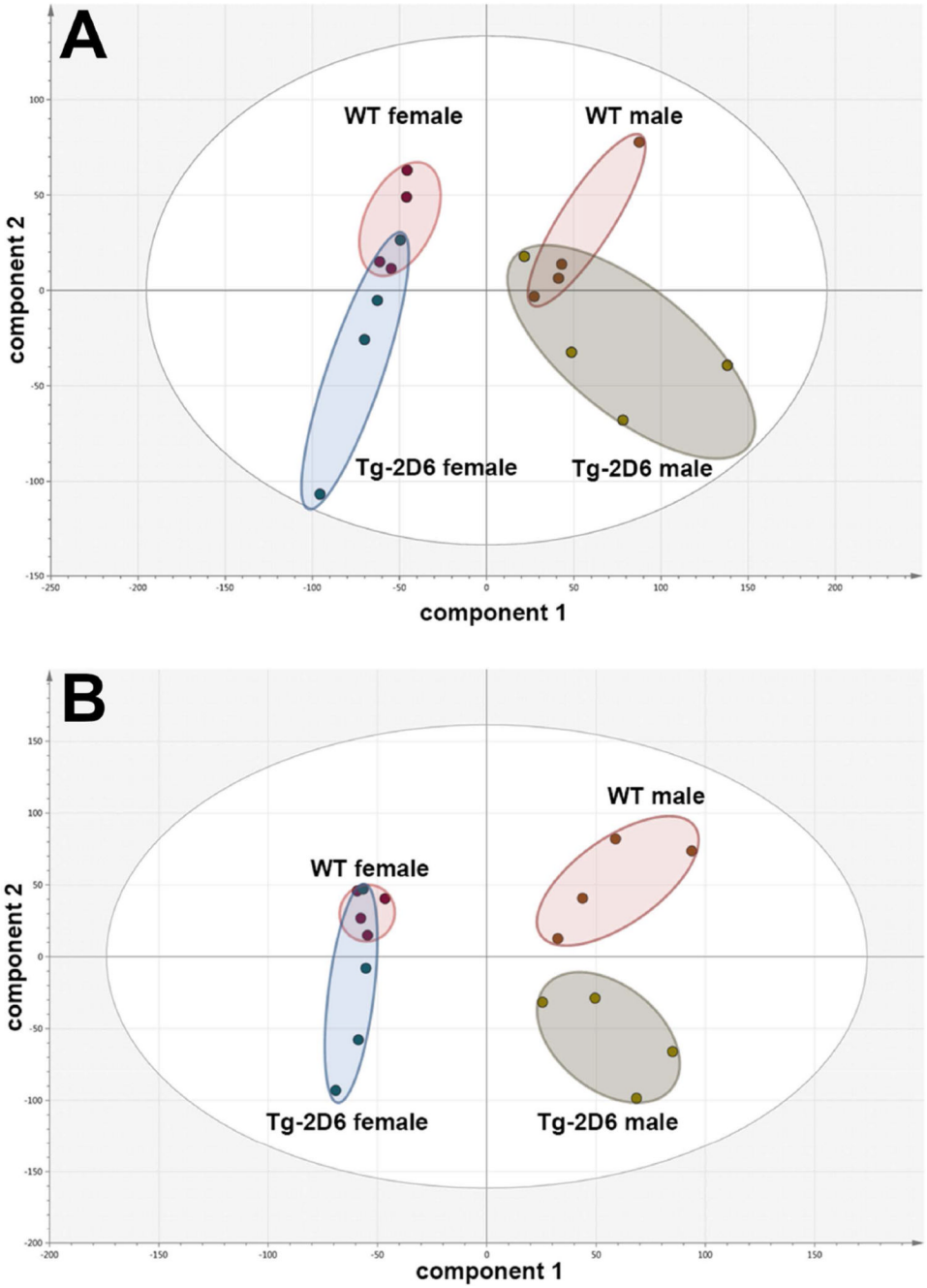

Figure 1.

Principal components analysis (PCA) scores plots for urines of male and female WT and Tg-2D6 mice from UPLC-ESI-QTOFMS metabolomics in positive-ion mode. (A) Four of each of male WT, female WT, male Tg-2D6 and female Tg-2D6 mice were studied and their 0–24h urines subjected to UPLC-ESI-QTOFMS analysis. For both male and female mice, there was poor clustering and considerable overlap of the scores between the WT and Tg-2D6 mice. (B) Four of each of male WT, female WT, male Tg-2D6 and female Tg-2D6 mice were administered debrisoquine (10 mg/kg p.o.) and their 0–24h urines subjected to UPLC-ESI-QTOFMS analysis. In contrast to the urines from untreated animals, there was a clear separation of scores between the WT and Tg-2D6 male mice.

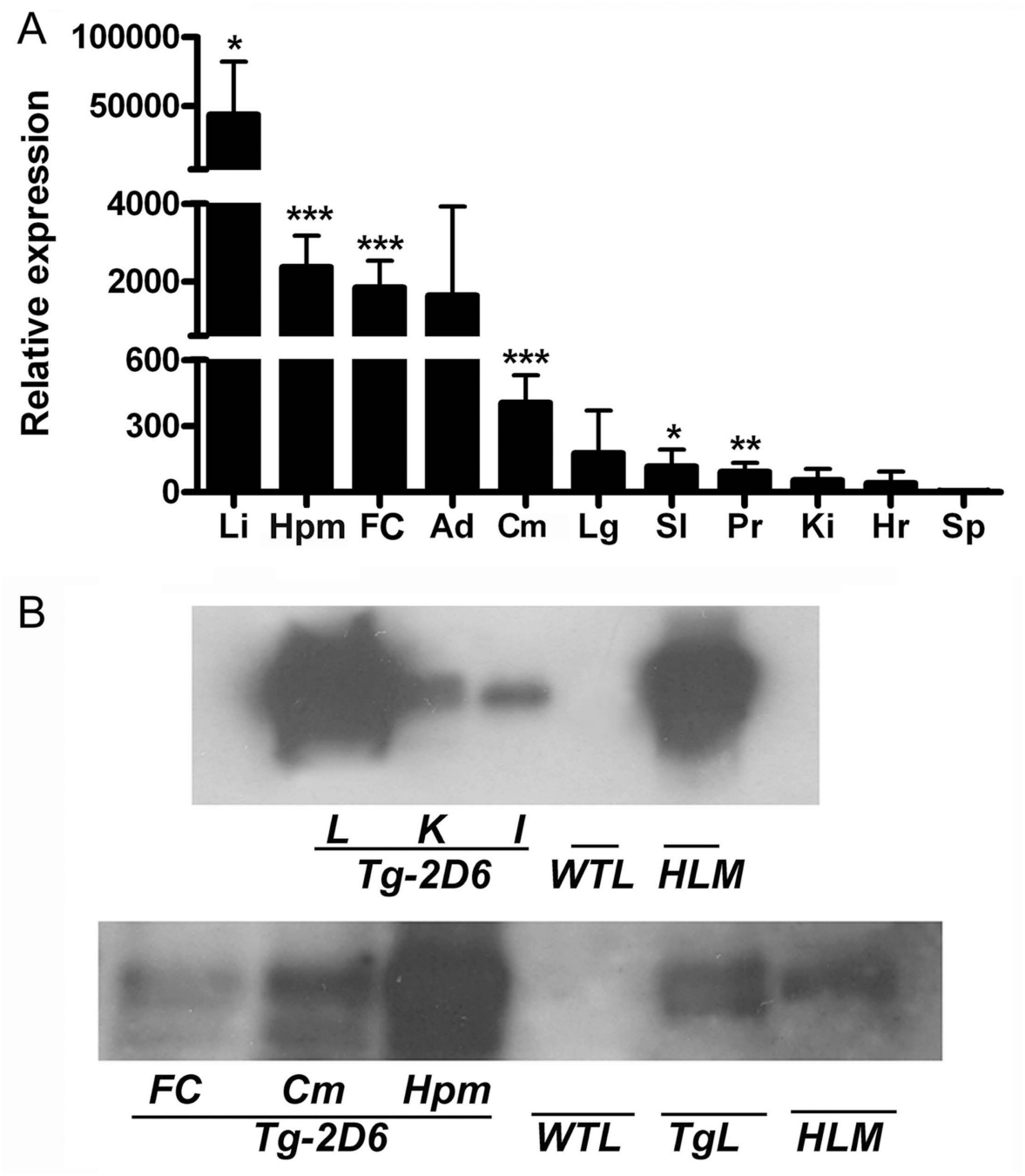

Figure 2.

CYP2D6 expression in liver and extrahepatic tissues of Tg-2D6 mice. (A) Fold CYP2D6 expression in each tissue was expressed relative to CYP2D6 in spleen. Lane Li, Hpm, FC, Ad, Cm, Lg, SI, Pr, Ki, Hr and Sp represented liver, hippocampus, frontal cortex, adrenal gland, cerebellum, lung, small intestine, prostate, kidney, heart, and spleen, respectively. The mean ± standard deviations are shown with n=6 (* for $P < 0.05$, ** for $P < 0.01$, *** for $P < 0.001$). (B) Western blot analysis of CYP2D6 in liver, kidney, intestine and brain regions from Tg-2D6 mice and WT mice. Upper panel: each lane was loaded with 20 μg of microsomal protein pooled from three mice for liver (L), kidney (K) intestine (I) from Tg-2D6 and WT mice, and human liver microsomes (HLM). Lower panel: each lane was

loaded with 100 μg of microsomal protein from FC, Cm, and Hpm, and 20 μg of protein for WTL, TgL and HLM pooled from three mice..

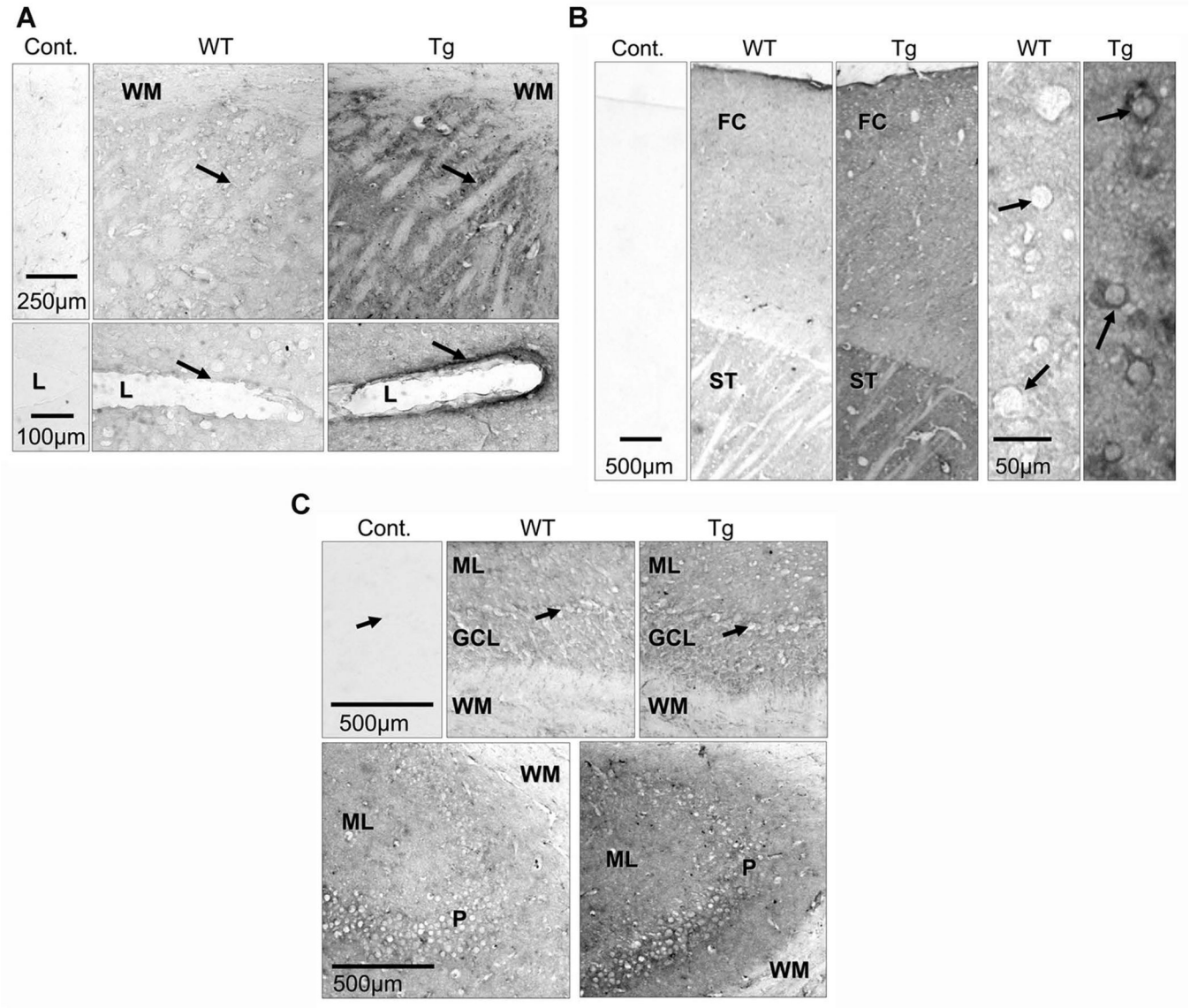

Figure 3.

Immunohistochemistry analysis of CYP2D6 expression in brain sections of Tg-2D6 and WT mice. (A) In transgenic mice there is strong immunostaining in cytoplasmic bridges (arrows) in the striatum, compared to WT mice. There is no immunostaining in the white matter (WM) in either strain of mice. The endothelial lining (arrows) of blood vessels in the striatum are strongly immunostained in transgenic mice but unstained in WT mice. L-lumen of blood vessel. (B) CYP2D immunostaining is higher in frontal cortex (FC) and striatum (ST) of transgenic compared to WT mice. There is no immunostaining in control sections incubated without primary antibody. In parietal cortex of transgenic mice, pyramidal cells (arrows) show strong CYP2D6 immunoreactivity, and this is absent in these cells in WT mice. (C) The molecular (ML) and granular cell layers (GCL) of the cerebellum are moderately more immunostained in transgenic compared with wild-type mice (top panels). The white matter (WM) and Purkinje cells (arrows) are unstained in both strains of mice. The bottom panels show that the hippocampus molecular (ML) and pyramidal (P) layers are moderately more immunoreactive in transgenic compared to WT mice; there is no

immunostaining in the white matter (WM). Cont: control section, WT: WT mice, Tg: Tg-2D6 mice.

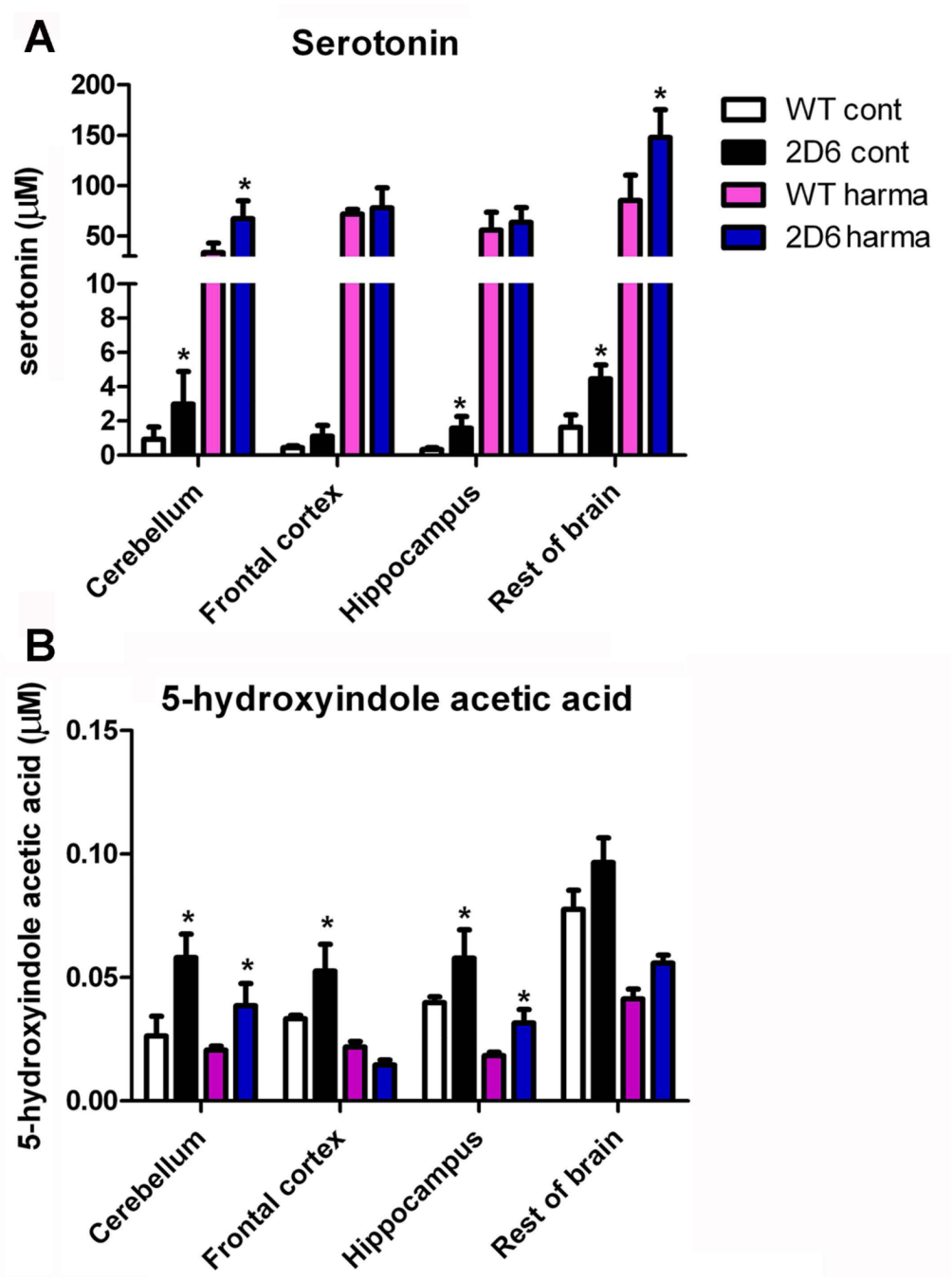

Figure 4.

Abundance of serotonin and its metabolite in brain of Tg-2D6 mice and WT mice. Abundance of serotonin in cerebellum, hippocampus, and rest of brain of Tg-2D6 is significantly higher than that in relative brain parts of WT mice (A). 5-hydroxyindoleacetic acid (5-HIAA) exhibited higher abundance in cerebellum, hippocampus, frontal cortex as well as rest of brain in Tg-2D6 mice than that in WT mice (B). Besides, harmaline administration enhanced the abundance of serotonin massively by 20–30 fold compared to control, while has decreasing effect on 5-HIAA abundance in brain. Similarly, serotonin in cerebellum and rest of brain of Tg-2D6 is significantly higher than that in relative brain parts of WT mice with harmaline induction, associated with higher level of 5-HIAA in cerebellum

and hippocampus of Tg-2D6 compared to WT mice (A, B). The mean ± standard deviations are shown with n=6 (* for $P < 0.05$).

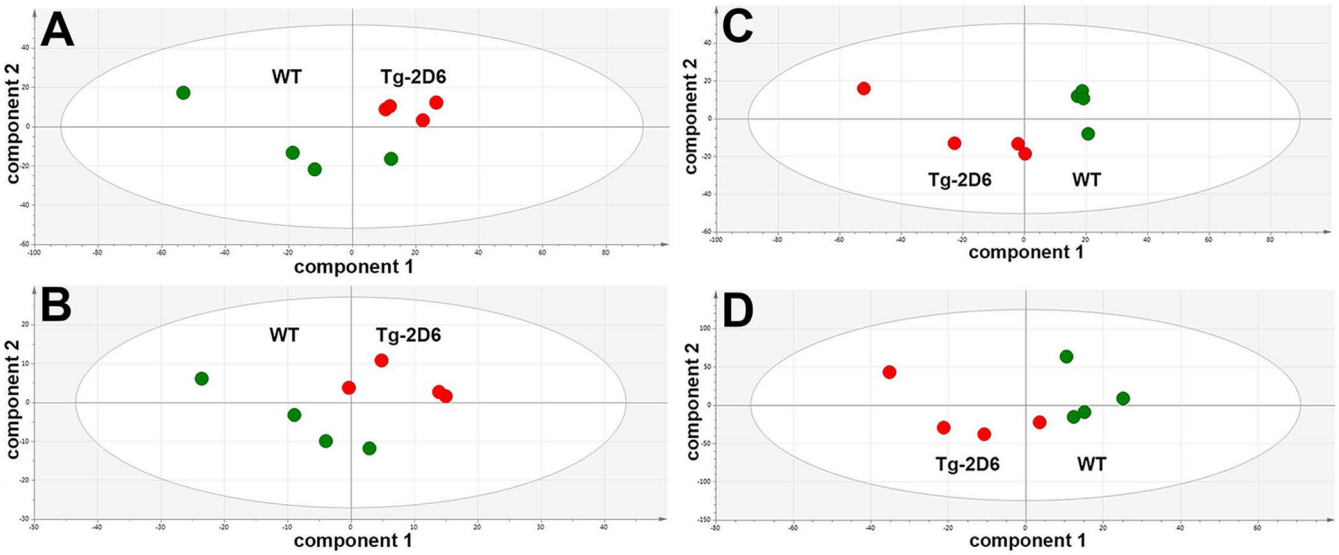

Figure 5.

Projection to latent structures-discriminant analysis (PLS-DA) scores plots for brain homogenates and cerebrospinal fluid (CSF) of male WT and Tg-2D6 mice from UPLC-ESI-QTOFMS metabolomics in electrospray positive- (ESI+) and negative-ion (ESI−) modes. Green circles represent WT mice (n=4) and red circles represent Tg-2D6 mice (n=4). (A) Brain homogenate in ESI+ mode. (B) Brain homogenate in ESI− mode. (C) CSF in ESI+ mode. (D) CSF in ESI− mode. In all cases A–D, Tg-2D6 and WT scores clustered and separated, indicating that the *CYP2D6* transgene had a significant impact of both brain and CSF metabolomes.

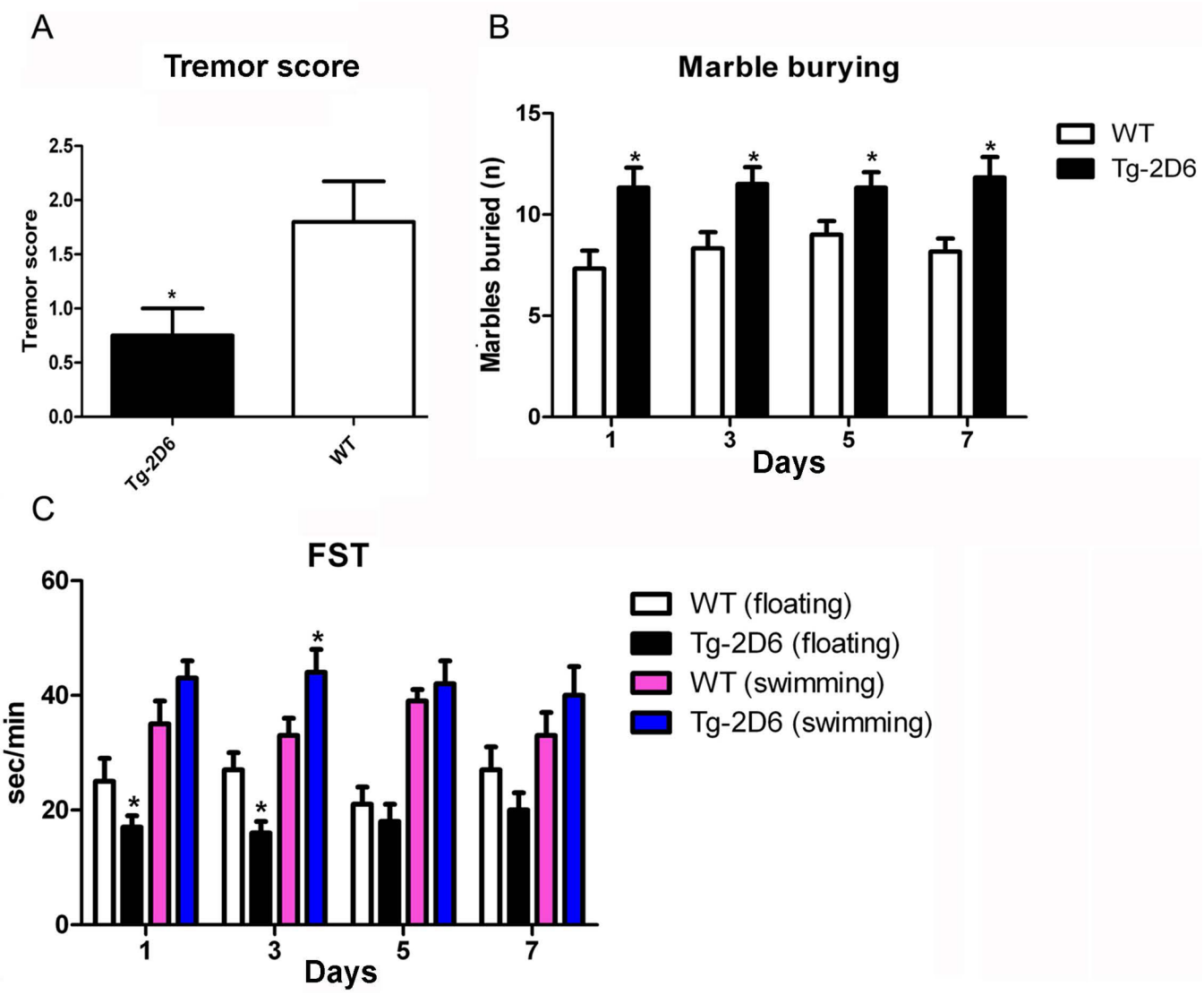

Figure 6.

Behavioral assays of Tg-2D6 and WT mice. (A) The results revealed that lower tremor score in Tg-2D6 mice is produced compared to WT mice which might be attributed to higher serotonin amount in brain (n=10). In addition, the behavior despair tests include marble burying assay and forced swimming test (FST) assay revealed that Tg-2D6 mice produce more buried marble (n=10) (B) as well as longer swimming time and less floating time (n=15) (C) in the containers compared to WT mice. The marble burying assay and FST assay were preformed in 1, 3, 5, 7 days. The mean + standard deviations are shown with n=10 for harmaline-induced tremor and marble burying assay, and n=15 for FST assay (* for $P < 0.05$).

Table 1

Molecules in mouse brain homogenate associated with CYP2D6

p(corr)[1]	retention time (min)	m/z	adduct identified	mass error (ppm)	molecule	pathway involved	P value
UP IN Tg-2D6 MOUSE							
0.92	0.33	220.119	[M+H]+	4	pantothenic acid	β-oxidation	<0.0001
0.92	0.29	162.111	[M+H]+	9	L-carnitine	FA transport into mitochondria for β-oxidation	0.0001
0.83	0.31	204.122	[M+H]+	5	acetyl-L-carnitine	transports carnitine out of mitochondria	0.0018
UP IN WT MOUSE							
No molecules statistically significantly elevated in WT mouse							

Table 2

Molecules in mouse cerebrospinal fluid associated with CYP2D6

p(corr)1	retention time (min)	m/z	adduct identified	mass error (ppm)	molecule	pathway involved	P value
UP IN Tg-2D6 MOUSE							
0.90	0.32	386.0149	[M−H]−	2	dCDP	pyrimidine metabolism [KEGG00240]	0.015
0.78	1.81	221.1115	[M+H]+	7	*N*-acetylglucosaminyl-amine	glycosyl-asparaginase [EC 3.5.1.26]	0.007
0.73	5.57	374.3033	[M+Na]+	0	anandamide	neuro-transmitter [CNS CB1 receptors]	0.038
0.72	0.28	162.1125	[M+H]+	0	L-carnitine	FA transport into mitochondria for β-oxidation	0.018
0.67	0.30	226.9968	[M+Cl]−	1	citric acid	Krebs cycle	0.025
0.66	0.29	215.0319	[M+Cl]−	4	$C_6H_{12}O_6$ (for example, inositol, glucose, fructose or galactose)		0.025
UP IN WT MOUSE							
0.88	4.87	428.3731	[M+H]+	0	stearoyl-L-carnitine	FA transport into mitochondria for β-oxidation	0.0006
0.79	2.87	343.0129	[M+Cl]−	7	dUMP	pyrimidine metabolism [KEGG00240]	N.S.